Research Article

Pulmonary Circulation

Products of oxidative stress and transient receptor potential ankyrin A1 expression in the brainstem after lung ischemia–reperfusion injury

Xiaoying Gu[1], Yu Nan[2], Xiaochuan Pang[3], Wenwen Zhang[1], Jian Zhang[1] and Yiyuan Zhang[1]

[1]Department of Anesthesiology, The First Hospital of Jilin University, Changchun, China; [2]Department of Gynecology and Obstetrics, The Second Hospital of Jilin University, Changchun, China; [3]Clinical Laboratory, The First Hospital of Jilin University, Changchun, China

Abstract

Lung ischemia–reperfusion injury is a common clinical concern. As the injury occurs, the pulmonary afferent nerves play a key role in regulating respiratory functions under pathophysiological conditions. The present study was to examine products of oxidative stress and expression of transient receptor potential A1 in the commissural nucleus of the solitary tract after lung ischemia–reperfusion injury; and further to determine molecular mediators linking to activation of oxidative stress and transient receptor potential ankyrin A1. A rat model of lung ischemia–reperfusion injury was used. Enzyme-linked immunosorbent assay and western blot analysis were employed to examine products of oxidative stress (i.e. 8-isoprostaglandin F2α and 8-hydroxy-2′-deoxyguanosine), and expression of transient receptor potential A1, Nrf2-antioxidant response element, and NADPH oxidase. 8-isoprostaglandin F2α and 8-hydroxy-2′-deoxyguanosine were amplified in the commissural nucleus of the solitary tract of lung ischemia–reperfusion injury rats, accompanied with downregulation of Nrf2-antioxidant response element, and upregulation of NOX4 and transient receptor potential A1. Blocking NADPH oxidase (subtype NOX4) decreased products of oxidative stress in the commissural nucleus of the solitary tract and attenuated upregulation of transient receptor potential A1 induced by lung ischemia–reperfusion injury. Our data revealed specific signaling pathways by which lung ischemia–reperfusion injury impairs Nrf2-antioxidant response and activates oxidative stress in the brainstem thereby leading to amplification of transient receptor potential A1 receptor likely via products of oxidative stress. Data suggest the abnormalities in the pulmonary afferent signals at the brainstem level which is likely to affect respiratory functions as lung ischemia–reperfusion injury occurs.

Keywords

transient receptor potential A1, oxidative stress, lung ischemia, brainstem, afferent nerves

Date received: 1 March 2019; accepted: 27 June 2019

Pulmonary Circulation 2019; 9(3) 1–9
DOI: 10.1177/2045894019865169

Introduction

Lung ischemia–reperfusion injury (LIRI) is a common and severe postoperative complication that often occurs after lung transplantation, cardiopulmonary bypass, cardiopulmonary resuscitation, pulmonary embolism, and sepsis.[1,2] Although surgical technology is developed, an inevitable surge in LIRI has been seen in clinics due to its wide application. The underlying mechanisms leading to LIRI are primarily due to oxidative stress, inflammation, cellular apoptosis, intracellular calcium overload, etc.[3] Nonetheless, it is noteworthy to determine central molecular mediators and their signal pathways involved in pathophysiological process of LIRI.

Transient receptor potential ankyrin 1 (TRPA1) plays a functional role in regulating neurogenic inflammation resulting from channel activation to a variety of compounds including pungent agents, irritant chemicals, reactive

The first two authors contributed equally to this paper.

Corresponding authors:
Jian Zhang and Yiyuan Zhang, Department of Anesthesiology, The First Hospital of Jilin University, 71 Xinmin Street, Changchun, Jilin 130021, China.
Email: zyj17871@163.com

oxygen, and products of oxidative stress-induced lipid peroxidation.[4–8] TRPA1 has been shown to appear in pulmonary sensory nerves and is engaged in development of inflammation-mediated responses and ischemic injury.[9–11] Recent findings further suggest that roles of proinflammatory cytokines (PICs) and oxidative stress in regulating TRPA1 functions in visceral and pulmonary sensory nerves and blocking PIC signals can decrease upregulation of TRPA1 expression in sensory nerves after inflammatory responses.[12–14]

Pulmonary sensory nerves play an essential role in regulating respiratory functions to maintain homeostasis.[15] A large subset of afferents in the vagus nerves respond to inflammatory mediators and oxidative stress and noxious stimuli.[15] Under pathophysiological conditions, stimulation of TRPA1 in a variety of sensory nerves has been reported to mediate neurogenic inflammatory responses.[12–14,16] In the process of stress response, the levels of PICs are increased and a number of receptors associated with PIC stimulation are upregulated in nodose ganglions (NGs).[17] Note that the NG neurons mainly supply sensory pulmonary vagal nerves and send sensory signals to the central nervous system in rats.

Sensory input from nerve endings in the lungs is mediated to vagal afferent neurons in the lower nodose and superior jugular ganglions. The NG is derived from epibranchial placodes and the jugular ganglions originate from the neural crest cells, which defines the phenotypes of the vagal fibers.[18] Primary respiratory vagal reflexes modifying the pattern of breathing are evoked via lung inflation and activation of chemoreceptors by chemical substances affecting vagal afferents.[15] The central endings of vagal afferent neurons innervating the airways terminate in the medulla oblongata (such as the commissural nucleus of the solitary tract (cNTS)) and release a variety of neurotransmitters and neuromodulators.[15] This thereby affects vagal motor neurons in the brainstem.

Thus, in the current study we hypothesized that LIRI leads to impairment of Nrf2-antioxidant response element (Nrf2-ARE) and Nrf2-regulated NADPH quinone oxidoreductase-1 (NQO1) in the cNTS of rats. Superoxide dismutase (SOD) is a class of enzymes to catalyze the dismutation of superoxide, whereas 8-isoprostaglandin F2α (8-iso PGF2α) is a product of oxidative stress and 8-hydroxy-2′-deoxyguanosine (8-OHdG) is a key biomarker of protein oxidation. We also hypothesized that LIRI inhibits SOD and amplifies oxidative NADPH oxidase (subtype NOX4) in the cNTS, and thereby increases 8-iso PGF2α and 8-OHdG and upregulates TRPA1 expression. We further hypothesized that blocking NOX4 decreases the levels of 8-iso PGF2α and 8-OHdG in the cNTS of LIRI rats and attenuates upregulation of TRPA1. In addition, we examined the role of PIC signals in engagement of TRPA1 expression.

Methods

Animal

All animal protocols were in accordance with the guidelines of the International Association for the Study of Pain and approved by the Animal Care and Use Committee of Jilin University. Male Sprague-Dawley (200–250 g) were housed in individual cages with free access to food and water and were kept in a temperature-controlled room (25°C) on a 12/12 h light/dark cycle.

Lateral ventricle cannulation

The rats were anesthetized with sodium pentobarbital (60 mg/kg body weight, i.p.) and immobilized in a stereotaxic apparatus (David Kopf, USA). After making a midline incision, the skull was exposed and one burr hole was drilled. Following this, animals were cannulated with an L-shaped stainless steel cannula aimed at the lateral ventricle according to the coordinates: 3.7 mm posterior to the bregma, 4.1 mm lateral to the midline, and 3.5 mm under the dura. The guide cannula was fixed to the skull using dental zinc cement.

A model of LIRI and administration of drugs

The rats were initially anesthetized using pentobarbital sodium (60 mg/kg, i.p.) and then anesthesia was maintained by continuous infusion of pentobarbital (0.05 mg/kg/min). An endotracheal tube was inserted and the rats were ventilated using a rat ventilator (Harvard Apparatus, Boston, MA). The ventilating parameters were set with an inspiratory oxygen fraction (FiO_2) of 40% at a rate of 50–60 breaths/min and a tidal volume of 6–8 ml/kg.

Catheters were inserted into the femoral artery and vein for monitoring arterial blood pressure and administration of fluids (saline, 1 ml/h) and drugs (vecuronium bromide, 0.1 mg/kg/h; heparin, 250 U/kg), respectively. A left anterolateral thoracotomy was performed in the fifth intercostal space, and the pleura was exposed to allow the left hilum of the lung to be isolated. After stabilizing for 15 min, the tidal volume was decreased to 5–7 ml/kg, and the rate was increased to 70–75 breaths/min. Lung ischemia was induced by clamping the left pulmonary hilum, including the left main bronchus, artery, and vein, for 1 h, followed by reperfusion induced by removing the clamp and ventilating the left lung for 5 h. The sham control group (“sham control”) underwent the left thoracotomy without clamping hilus and was ventilated for 6 h. In addition, healthy and body weight-matched control rats (that did not receive any surgical manipulation; “control”; n = 6) were included.

The thoracic incision was protected from evaporative losses using a covering of wet absorbent gauze. The body heat of the rats was maintained using a heating lamp at

a rectal temperature within the normal range (36–37°C). Arterial blood (0.3 ml) was collected from each rat before induction of ischemia and 30 min and 2.5 and 5 h after reperfusion, and then blood gas analyses were performed (ABL 800; Radiometer, Copenhagen, Denmark). Arterial partial pressure of oxygen (PaO_2) and arterial partial pressure of carbon dioxide ($PaCO_2$) were also recorded. The arterial pressure, heart rate, and temperature of each rat were also monitored continuously throughout the study.

In subgroups of experiments, the later ventricular cannula was connected to a perfusion pump with polycarbonate tubing. The pump was used to deliver NOX4 inhibitor GKT137831 (10 μg, Cayman Chem. Co.) for a period of 5 h at a rate at 1 μl/h. This intervention allowed animals to receive continuous intracerebroventricular (ICV) infusion following the LIRI. In the same way, IL-1Ra (IL-1R receptor inhibitor; Sigma-Aldrich), tocilizumab (TCZB, IL-6R inhibitor; Selleckchem Co.), and etanercept (ETAN, TNF-α receptor inhibitor; Sigma-Aldrich) were given, respectively, via ICV (10 μg/each inhibitor). At the end of the experiment, the rats were euthanized with pentobarbital sodium (120 mg/kg, i.p.), and the brainstem was taken out.

ELISA measurement

The cNTS tissues of the rats were obtained under an anatomical microscope. All the tissues from individual rats were sampled for the analysis. Total protein was then extracted by homogenizing the sample in ice-cold immunoprecipitation assay buffer with protease inhibitor cocktail kit. The lysates were centrifuged and the supernatants were collected for measurements of protein concentrations using a bicinchoninic acid assay reagent kit. The levels of 8-iso PGF2α and 8-OHdG were examined using ELISA assay kits (obtained from Promega Co. and Abcam Co.) according to the provided description. Briefly, polystyrene 96-well microtiter immunoplates were coated with affinity-purified rabbit primary antibodies. Parallel wells were coated with purified rabbit IgG for evaluation of nonspecific signal. After overnight incubation, plates were washed. Then, the diluted samples and 8-iso PGF2α/8-OHdG standard solutions (100 pg/ml–100 ng/ml) were distributed in each plate. The plates were washed and incubated with anti-8-iso PGF2α/8-OHdG galactosidase. Then, the plates were washed and incubated with substrate solution. After incubation, the optical density was measured using an ELISA reader. In the similar way, the levels of IL-1β, IL-6, and TNF-α were also determined using ELISA assay kits (Wuhan Fine Biotech Co).

Western blot analysis

Briefly, the cNTS tissues were removed and total protein was extracted. The lysates were centrifuged and the supernatants were collected. After being denatured, the supernatant samples containing 20 μg of protein were loaded onto gels and electrically transferred to a polyvinylidene fluoride membrane. The membrane was incubated with respective primary antibodies (at 1:500, Abcam and/or Antibodies online Com): rabbit anti-Nrf2, anti-NQO1, anti-SOD, anti-NOX1/anti-NOX2/anti-NOX3/anti-NOX4, and anti-TRPA1. The membranes were washed and incubated with an alkaline phosphatase conjugated anti-rabbit secondary antibody (1:1000). The immunoreactive proteins were detected by enhanced chemiluminescence. The bands recognized by the primary antibody were visualized by exposure of the membrane onto an X-ray film. The membrane was stripped and incubated with anti-β-actin to show equal loading of the protein. Then, the film was scanned and the optical densities of primary antibodies and β-actin bands were determined using the Scion Software. Values for densities of immunoreactive bands/β-actin band from the same lane were determined. Each of the values was then normalized to a control sample.

Statistical analysis

All data were analyzed using one-way repeated-measures analysis of variance. Values were presented as means ± standard error of mean. For all analyses, differences were considered significant at $P < 0.05$. All statistical analyses were performed by using SPSS for Windows version 13.0 (SPSS Inc.).

Results

Blood gas and arterial blood pressure

The arterial-alveolar oxygen pressure gradient ($A\text{-}aDO_2$) was calculated using the following formula: $A\text{-}aDO_2 = \text{fraction inspired } O_2 \times (Patm\text{-}PH_2O) - (PaCO_2/RQ) - PaO_2$, where $Patm = 760$ mmHg, $PH_2O = 47$ mmHg, and $RQ = 0.8$. In sham controls ($n = 32$), no significant differences in PaO_2 and $A\text{-}aDO_2$ were observed over baseline at any time point (Fig. 1(a) and (b)). Figure 1(a) and (b) further shows that in LIRI group ($n = 45$), PaO_2 decreased by 24% (30 min post-reperfusion) and by 13% (5 h post-reperfusion) as compared with baseline ($P < 0.05$ versus baseline), whereas the $A\text{-}aDO_2$ increased by 23% (30 min post-reperfusion) and by 12% (5 h post-reperfusion) ($P < 0.05$ versus baseline). An exacerbated blood gas exchange with declined PaO_2 and elevated $A\text{-}aDO_2$ indicated the process of LIRI in our rat model used in this study. In addition, the levels of $PaCO_2$ and the ratio of PaO_2 to FiO_2 were shown in Tables 1 and 2, respectively.

Arterial blood pressure and heart rate were stable throughout the whole study in sham control rats (Fig. 1(c) and (d)). Although the mean arterial pressure (MAP)

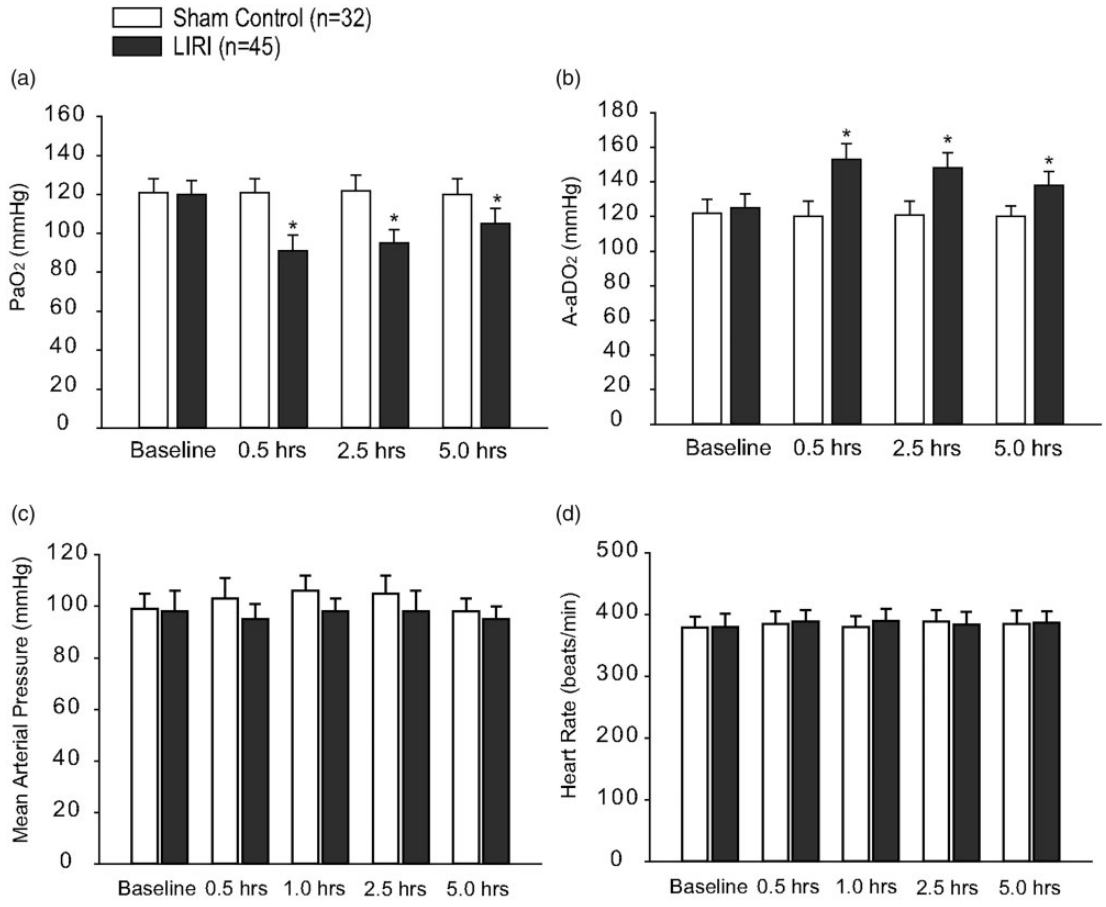

Fig. 1. Blood oxygen and carbon dioxide; and blood pressure and heart rate after lung ischemia reperfusion injury (LIRI). (a and b): Arterial PaO_2 and arterial $PaCO_2$ of rats in sham control rats and rats with LIRI. Baseline indicates before ischemia; and 0.5, 2.5, and 5.0 h indicate times after reperfusion. *$P < 0.05$ versus baseline. (c and d): MAP and heart rate of sham control rats and LIRI rats before ischemia, and 0.5–5.0 h after reperfusion. There were no differences in MAP and heart rate for baseline and at different time points after reperfusion in sham control and LIRI groups. Note that "n" indicates a total number of rats in sham control group and LIRI group used in the present study. LIRI: lung ischemia–reperfusion injury.

Table 1. The levels of blood $PaCO_2$ (mmHg) in sham control rats and rats with LIRI.

	Baseline	0.5 h	2.5 h	5 h
Sham control	35.21 ± 3.7	36.45 ± 4.5	35.57 ± 5.5	37.23 ± 4.6
LIRI	33.26 ± 3.3	34.38 ± 4.1	35.32 ± 4.3	35.16 ± 3.2

LIRI: lung ischemia–reperfusion injury; $PaCO_2$: partial pressure of carbon dioxide.
There were no significant differences in $PaCO_2$ for baseline and 0.5–5 h after LIRI between two groups ($P > 0.05$ sham control versus LIRI for each time point).

Table 2. The ratio of PaO_2 to FiO_2.

	Baseline	0.5 h	2.5 h	5 h
Sham control	303 ± 22	303 ± 18	305 ± 21	300 ± 17
LIRI	300 ± 24	$228 \pm 20^{*,\dagger}$	$238 \pm 18^{*,\dagger}$	$263 \pm 19^{*,\dagger}$

FiO_2: inspiratory oxygen fraction; LIRI: lung ischemia–reperfusion injury; PaO_2: partial pressure of oxygen.
The ventilating parameters were set with an inspiratory oxygen fraction (FiO_2) of 40%. A smaller ratio was observed 0.5–5 h after LIRI as compared with baseline and with different time points in sham control group.
*$P < 0.05$ versus baseline; $^{\dagger}P < 0.05$ versus sham control.

appeared to slightly decrease in LIRI rats, no significance difference was seen between sham control group and LIRI group (i.e. MAP: 98 ± 5 mmHg in sham control and 95 ± 6 mmHg in LIRI 5 h post-reperfusion; $P > 0.05$ between two groups). There was no significant difference in heart rate between the two groups at any time point (i.e. 385 ± 10 beats/min in sham control group and 387 ± 12 beats/min in LIRI group 5 h after reperfusion; $P > 0.05$ between two groups).

Expression of Nrf2-ARE and SOD

We first examined the protein levels of Nrf2 and Nrf2-regulated NQO1 in the cNTS. Figure 2(a) shows that the

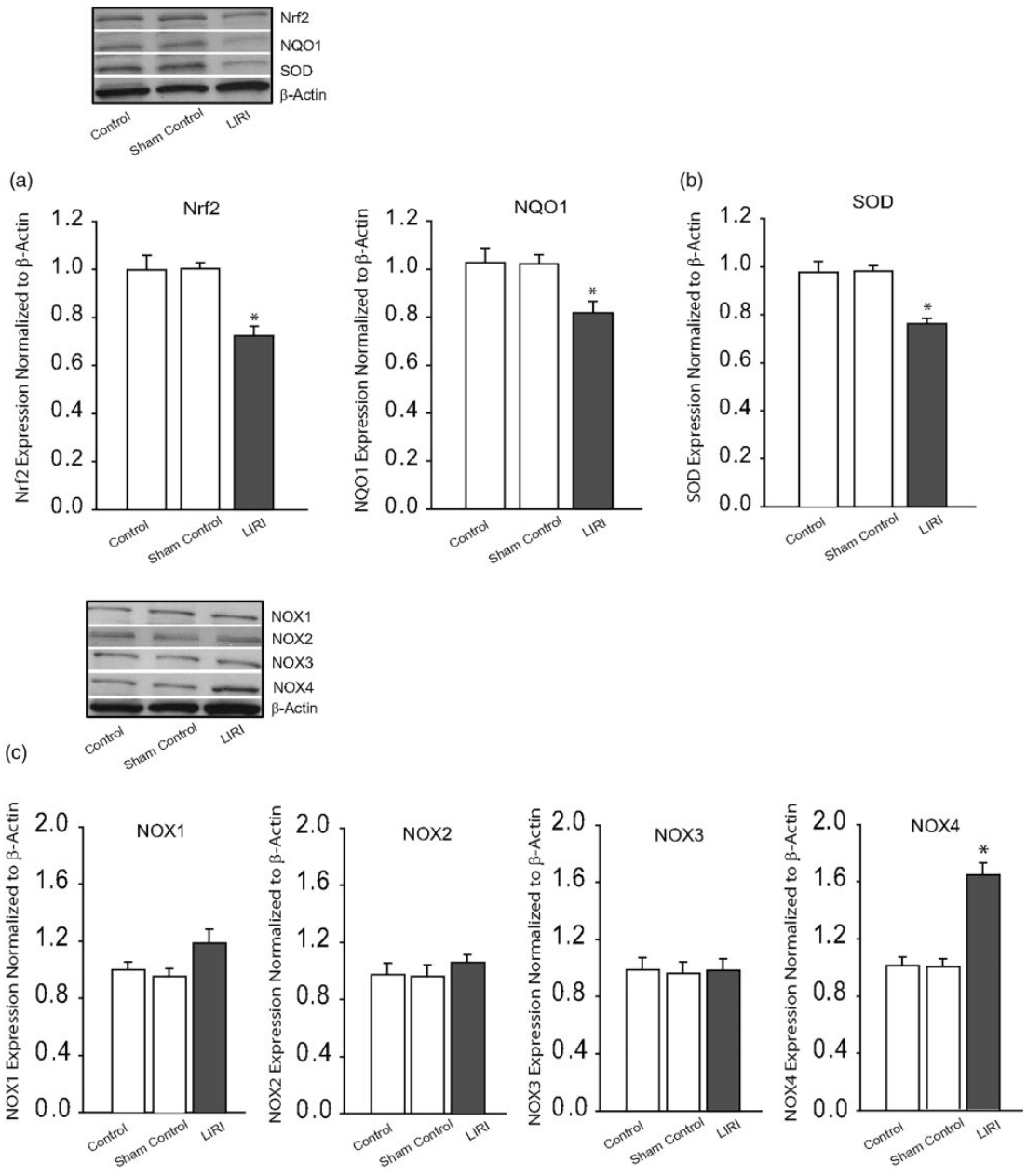

Fig. 2. Effects of LIRI on antioxidant response and oxidative stress signal pathways. (a and b): Protein expression levels of Nrf2-ARE and SOD. Top panel and bottom panel are representative bands and averaged data: Nrf2/NQO1 and SOD were decreased in the cNTS of LIRI rats. $^*P < 0.05$, LIRI rats versus control rats and sham control rats. n = 6–12 in each group. Insignificant difference was seen between control rats and sham control rats ($P > 0.05$). (c) Representative bands and averaged data showing that protein expression levels of NOX1, NOX2, and NOX3 were not altered significantly by LIRI, but NOX4 was amplified by LIRI. $^*P < 0.05$, LIRI rats versus control rats and sham control rats. n = 6–10 in each group. Insignificant difference was seen between control rats and sham control rats ($P > 0.05$). SOD: superoxide dismutase.

protein expression levels of Nrf2 and Nrf2-regulated NQO1 were decreased in the cNTS of LIRI rats ($P < 0.05$, LIRI rats versus control rats; n = 8–12). Likewise, Fig. 2(b) further shows that LIRI led to down-regulation of SOD expression in the cNTS ($P < 0.05$, LIRI rats/n = 8 versus controls rats/n = 6 and sham control rats/n = 8).

Expression of NADPH oxidases (NOXs)

We have then examined the protein levels of NOX1, NOX2, NOX3, and NOX4 in the cNTS of LIRI rats, sham control rats, and control rats. Figure 2(c) shows that no significant differences in expression of NOX1, NOX2, and NOX3 were observed among three groups ($P > 0.05$, LIRI rats versus

control rats and sham control rats for each of NOXs; n = 6–8 in each group). In contrast, NOX4 in the cNTS was amplified by LIRI as shown in Fig. 2(c) ($P < 0.05$, LIRI rats/n = 10 versus control rats/n = 6 and sham control rats/n = 8).

Products of oxidative stress and expression of TRPA1

We further examined products of oxidative stress in the cNTS of LIRI rats and sham control rats as shown in Fig. 3(a). This figure demonstrates that 8-iso PGF2α and 8-OHdG were increased in the cNTS of LIRI rats (n = 16) as compared with sham control rats (n = 15; $P < 0.05$, LIRI versus controls). In addition, ICV infusion of NOX4 inhibitor GKT137831 attenuated increases of both 8-iso PGF2α and 8-OHdG in the cNTS ($P < 0.05$, LIRI rats versus LIRI rats with infusion of inhibitor/n = 12). Note that no significant differences in 8-iso PGF2α and 8-OHdG were observed between sham control rats and control rats ($P > 0.05$).

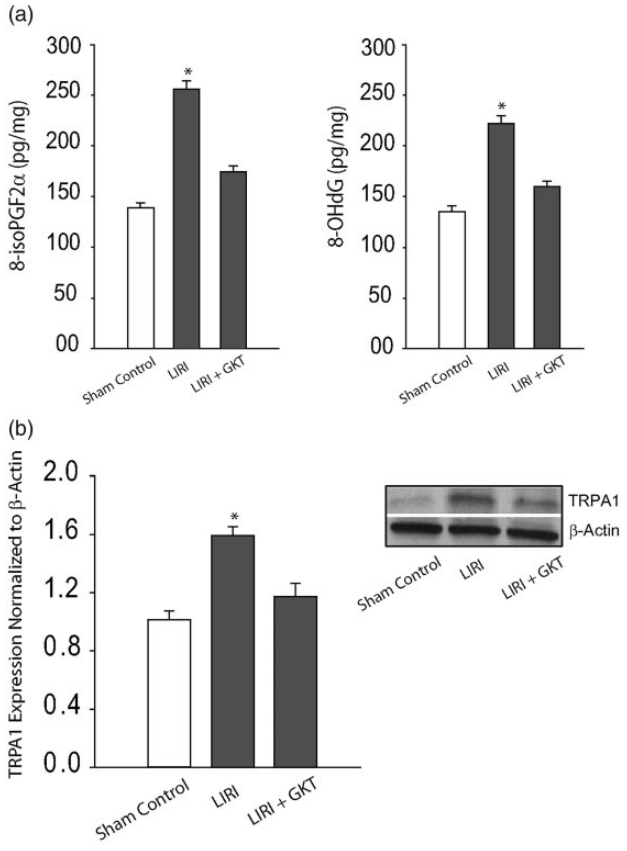

Fig. 3. Effects of NOX4 on products of oxidative stress and expression of TRPA1. (a) LIRI amplified the levels of oxidative products 8-iso PGF2α and 8-OHdG in the cNTS. As NOX-4 inhibitor GKT137831 (GKT) was infused via ICV, increases of 8-iso PGF2α and 8-OHdG were attenuated. *$P < 0.05$, LIRI rats (n = 16) versus sham control rats (n = 15) and LIRI rats with inhibitor (n = 12). (b) The protein levels of TRPA1 were amplified in the cNTS tissues of LIRI rats and inhibition of NOX4 by ICV administration of GKT137831 decreased expression of TRPA1 in the cNTS of LIRI rats. *$P < 0.05$, LIRI rats (n = 12) versus sham control rats (n = 8) and LIRI rats with inhibitor (n = 10). GKT: GKT137831; LIRI: lung ischemia–reperfusion injury; TRPA1: transient receptor potential ankyrin 1.

Figure 3(b) demonstrates that LIRI upregulated protein expression of TRPA1 receptors in the cNTS and ICV infusion of GKT137831 significantly attenuated amplification of TRPA1 induced by LIRI ($P < 0.05$, LIRI rats versus sham control rats and LIRI rats with inhibitor; n = 8–12 in each group).

Levels of PICs and effects of PIC inhibition on TRPA1 expression

In order to determine if PIC signal was involved in the effects of LIRI, in additional experiments, we examined the levels of PICs in the cNTS. First, there were insignificant differences in the levels of PICs between sham control rats and control rats ($P > 0.05$). Figure 4(a) further shows that IL-1β, IL-6, and TNF-α were significantly increased in the cNTS of LIRI rats ($P < 0.05$ versus sham control rats; n = 12 in each group) as compared with sham control rats. Furthermore, ICV infusion of NOX4 inhibitor GKT137831 did not alter amplifications of PICs in the cNTS evoked by LIRI. Insignificant differences in the levels of IL-1β, IL-6, and TNF-α in the cNTS were observed between LIRI rats with ICV infusion of inhibitor (n = 8) and LIRI rats (n = 12; $P > 0.05$, between two group). In contrast, Fig. 4(b) demonstrates that blocking PIC signals by respective ICV infusion of IL-1Ra, TCZB, and ETAN attenuated upregulation of TRPA1 in the cNTS induced by LIRI ($P < 0.05$, LIRI rats versus sham control rats and LIRI rats with each inhibitor; n = 6–10 in each group).

Discussion

In involvement of respiratory vagal reflexes, the cNTS can receive afferent inputs from the central endings of vagal sensory neurons innervating the airways and modify the pattern of breathing and thereby affect vagal motor neurons in the brainstem.[15] In the present study, we first examined the effects of LIRI on antioxidant response and oxidative stress signal pathways in the cNTS and we found that the expression of Nrf2-ARE signal and SOD expression were downregulated in the cNTS of LIRI rats as compared with sham control rats. In addition, we demonstrated that LIRI upregulated expression of NOX4 in the cNTS. Thus, it is well reasoned that products of oxidative stress 8-iso PGF2α and 8-OHdG were increased in the cNTS by LIRI.

Nrf2 is a transcription factor and as a basic leucine zipper protein it regulates the expression of antioxidant proteins protecting against oxidative damage triggered by injury and inflammation.[19] Numerous drugs that stimulate the Nrf2 pathway were used for treatment of diseases caused by oxidative stress.[20] LIRI can lead to oxidative injuries and inflammation in ischemic tissues.[3] Prior studies have also suggested that ischemic injuries can impair Nrf2-ARE

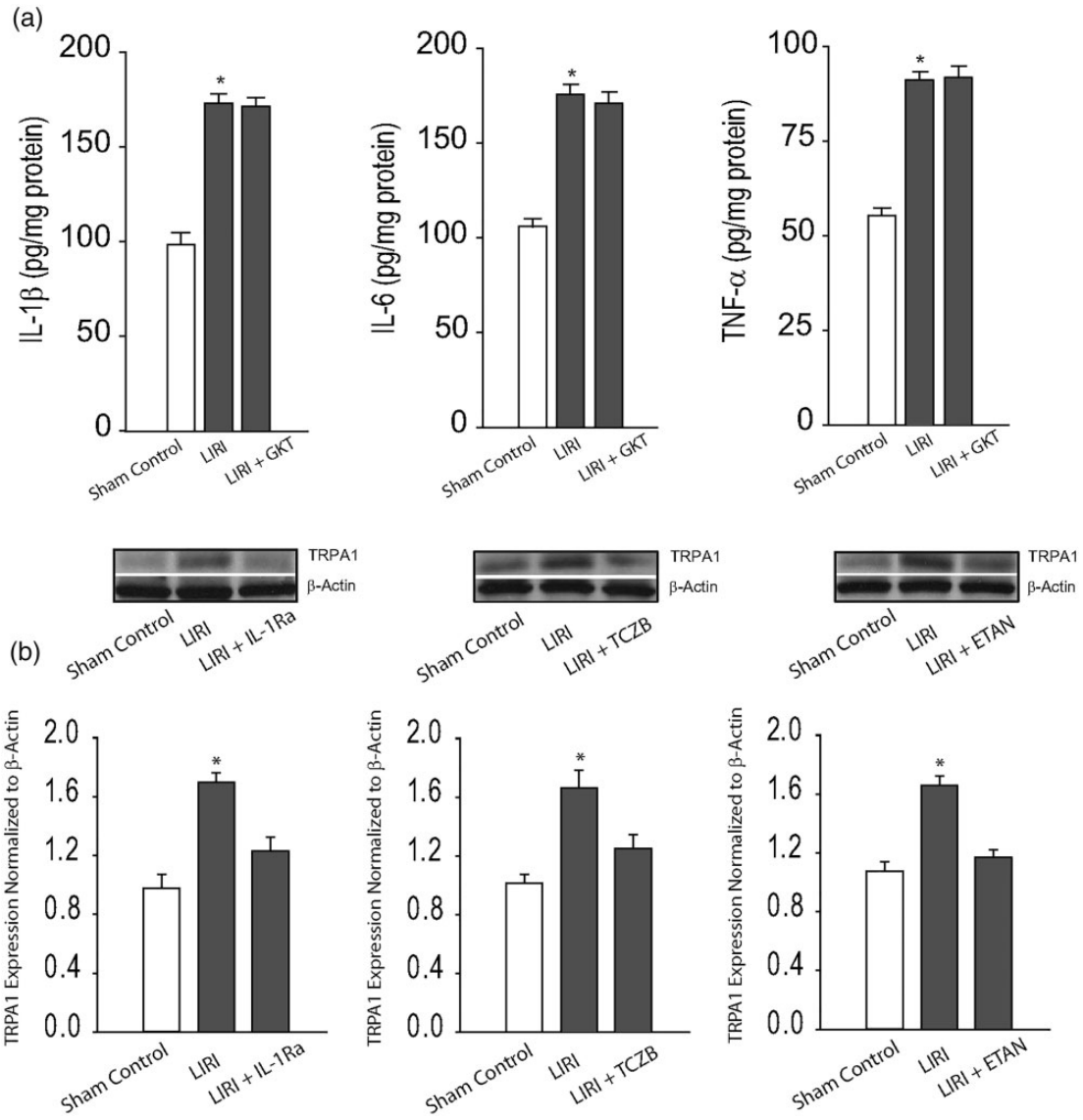

Fig. 4. Effects of NOX4 on PICs and effects of blocking PIC on TRPA1 expression. (a) LIRI amplified the levels of PICs (IL-1β, IL-6, and TNF-α) in the cNTS as compared with sham controls. *$P < 0.05$, LIRI rats (n = 12) versus sham control rats (n = 12). However, inhibition of NOX4 by ICV administration of GKT137831 (GKT) did not alter significantly the amplified levels of IL-1β, IL-6, and TNF-α in the cNTS of LIRI rats (n = 8). $P > 0.05$ between LIRI rats and LIRI rats with inhibitor. (b) Inhibition of PIC signals by respective ICV infusion of IL-1Ra (IL-1R inhibitor), TCZB (IL-6R inhibitor), and ETAN (TNFR inhibitor) attenuated upregulation of TRPA1 in the cNTS induced by LIRI. *$P < 0.05$, LIRI rats (n = 10) versus sham control rats (n = 6) and LIRI rats with each inhibitor (n = 8 in each group). ETAN: etanercept; GKT: GKT137831; IL-1Ra: IL-1R receptor inhibitor; LIRI: lung ischemia–reperfusion injury; TCZB: tocilizumab; TRPA1: transient receptor potential ankyrin 1.

signal pathways.[21] Under conditions of the oxidative stress, expression of Nrf2-ARE appears to be downregulated in central nerve tissues.[22] As shown in our current study, we also provided evidence that Nrf2-ARE signal was impaired in the cNTS during the process of LIRI. It is speculated that impaired Nrf2-ARE is likely to inhibit oxidative responses to a less degree in LIRI and thereby this links to increases of products of oxidative stress. It should be noted that accumulated evidence indicates that Nrf2-ARE is activated in an oxidative stress environment to play a neuroprotective role.[23]

TRPA1 activation can explain a wide variety of symptoms in patients suffering from asthma or other respiratory disorders and might also play a crucial role in infection-induced exacerbations. TRPA1 expression has been identified in bronchopulmonary vagal C-fiber afferents[24] and evidence for a role in asthma was provided.[25] In this prior study, it was demonstrated that airway hyper-reactivity as well as respiratory system inflammation was markedly reduced after genetic ablation of TRPA1 or after treatment with a TRPA1 antagonist. TRPA1 may represent one of the most promising targets for pharmaceutical interventions in

inflammatory respiratory diseases. To the best of our knowledge, there has not been any proof for a dysregulation of TRPA1 in the central regions innervating pulmonary vagal nerves following LIRI.

Our current data suggest that LIRI amplified expression of TRPA1 in the cNTS. Interestingly, inhibition of NOX4 attenuated the effects of LIRI on TRPA1 and this was linked to the inhibitory effects of NOX4 on products of oxidative stress 8-iso PGF2α and 8-OHdG. Of note, TRPA1 is responding to reactive oxygen species (ROS).[5,26–28] ROS are considered as endogenously generated molecule mediators during oxidative stress and/or inflammation.[5,26–28] It was speculated that increases of 8-iso PGF2α and 8-OHdG induced by LIRI upregulated TRPA1 expression in the cNTS. However, blocking NOX4 failed to attenuate increases of PICs in the cNTS induced by LIRI, suggesting that changes of PICs are independent of oxidative stress during LIRI per se. Nonetheless, our current data showed that blocking PIC receptor can attenuate TRPA1 expression in the cNTS. PICs including IL-1β, IL-6, and TNF-α have been reported to be involved in sensory vagal nerve-mediated reflex response.[29] A prior study has suggested that PICs and some receptors activated by PIC were increased in the NGs of rats with stress insult.[17] Taken together, the data suggest the role of TRPA1 in regulating vagal afferent inputs during the process of LIRI and products of oxidative stress and PICs are involved in activation of TRPA1, by which respiratory functions are likely to be adjusted to maintain homeostasis.

One source of ROS production is the enzyme family of NOX. The rodent genome encodes four genes that contain the catalytic NOX subunit, namely NOX1, NOX2, NOX3, and NOX4.[30] This electron-transferring subunit is constitutively inactive in resting cells and generates ROS after inflammatory stimuli.[31] While NOX2 activation is predominantly associated with innate immunity mediated host defense and NOX1 with blood pressure control and related vascular mechanisms,[32,33] NOX4 was shown highly expressed under ischemic conditions in the central nervous system.[34] Evidence has also identified activation of NOX4 as a causative factor that contributes to inflammatory role in the peripheral nervous system.[35] Nonetheless, in the current study we determined the effects of LIRI on expression levels of NOX1, NOX2, NOX3, and NOX4 in the cNTS of rats. We observed that NOX4 was upregulated among NOXs after LIRI. Our data suggest that LIRI leads to increases of ROS generation in the cNTS in addition to impairment of antioxidants and free radical scavengers.

In conclusion, LIRI impairs Nrf2-antioxidant response and Nrf2-regulated NQO1 in the cNTS of rats whereas LIRI can decrease SOD and amplify NOX4 in the cNTS. This process thereby leads to increases of products of oxidative stress 8-iso PGF2α and 8-OHdG in the cNTS. In addition, LIRI upregulates TRPA1 expression and increases the levels of PICs in the cNTS. Inhibition of oxidative stress signal by a NOX4 blocker attenuates TRPA1 expression with decreasing 8-iso PGF2α and 8-OHdG. A blockade of each PIC receptor also attenuates upregulation of TRPA1 expression induced by LIRI. We have revealed specific signaling pathways by which LIRI amplifies products of oxidative stress as well as PICs in the cNTS thereby leading to upregulation of TRPA1 receptor. Our data further suggest the abnormalities in the pulmonary afferent signals at the brainstem level which is likely to affect respiratory functions as LIRI occurs.

Authors' contribution

GX and NY performed the experiments and data analysis and they also drafted the paper; PX and ZW partly participated in performance of experiments and data analysis; and ZJ and ZY designed the experiments and performed data analysis and reviewed the paper. All the authors have reviewed and approved the paper.

Conflict of interest

The author(s) declare that there is no conflict of interest.

Funding

This research received no specific grant from any funding agency in the public, commercial, or not-for-profit sectors.

References

1. Ailawadi G, Lau CL, Smith PW, et al. Does reperfusion injury still cause significant mortality after lung transplantation? *J Thorac Cardiovasc Surg* 2009; 137: 688–694.
2. Rubenfeld GD, Caldwell E, Peabody E, et al. Incidence and outcomes of acute lung injury. *N Engl J Med* 2005; 353: 1685–1693.
3. Laubach VE and Sharma AK. Mechanisms of lung ischemia-reperfusion injury. *Curr Opin Organ Transplant* 2016; 21: 246–252.
4. Andersson DA, Gentry C, Moss S, et al. Transient receptor potential A1 is a sensory receptor for multiple products of oxidative stress. *J Neurosci* 2008; 28: 2485–2494.
5. Bandell M, Story GM, Hwang SW, et al. Noxious cold ion channel TRPA1 is activated by pungent compounds and bradykinin. *Neuron* 2004; 41: 849–857.
6. Bautista DM, Movahed P, Hinman A, et al. Pungent products from garlic activate the sensory ion channel TRPA1. *Proc Natl Acad Sci USA* 2005; 102: 12248–12252.
7. Jordt SE, Bautista DM, Chuang HH, et al. Mustard oils and cannabinoids excite sensory nerve fibres through the TRP channel ANKTM1. *Nature* 2004; 427: 260–265.
8. Sawada Y, Hosokawa H, Matsumura K, et al. Activation of transient receptor potential ankyrin 1 by hydrogen peroxide. *Eur J Neurosci* 2008; 27: 1131–1142.
9. Kwan KY, Allchorne AJ, Vollrath MA, et al. TRPA1 contributes to cold, mechanical, and chemical nociception but is not essential for hair-cell transduction. *Neuron* 2006; 50: 277–289.
10. Story GM, Peier AM, Reeve AJ, et al. ANKTM1, a TRP-like channel expressed in nociceptive neurons, is activated by cold temperatures. *Cell* 2003; 112: 819–829.
11. Lin YJ, Lin RL, Ruan T, et al. A synergistic effect of simultaneous TRPA1 and TRPV1 activations on vagal pulmonary C-fiber afferents. *J Appl Physiol* 2015; 118: 273–281.

12. Alvarenga EM, Souza LK, Araujo TS, et al. Carvacrol reduces irinotecan-induced intestinal mucositis through inhibition of inflammation and oxidative damage via TRPA1 receptor activation. *Chem Biol Interact* 2016; 260: 129–140.
13. Shi HL, Liu CH, Ding LL, et al. Alterations in serotonin, transient receptor potential channels and protease-activated receptors in rats with irritable bowel syndrome attenuated by Shugan decoction. *World J Gastroenterol* 2015; 21: 4852–4863.
14. Trevisan G, Benemei S, Materazzi S, et al. TRPA1 mediates trigeminal neuropathic pain in mice downstream of monocytes/macrophages and oxidative stress. *Brain* 2016; 139: 1361–1377.
15. Lee LY and Yu J. Sensory nerves in lung and airways. *Compr Physiol* 2014; 4: 287–324.
16. Poole DP, Amadesi S, Veldhuis NA, et al. Protease-activated receptor 2 (PAR2) protein and transient receptor potential vanilloid 4 (TRPV4) protein coupling is required for sustained inflammatory signaling. *J Biol Chem* 2013; 288: 5790–5802.
17. Steinberg BE, Silverman HA, Robbiati S, et al. Cytokine-specific neurograms in the sensory vagus nerve. *Bioelectron Med* 2016; 3: 7–17.
18. Undem BJ and Carr MJ. Pharmacology of airway afferent nerve activity. *Respir Res* 2001; 2: 234–244.
19. Moi P, Chan K, Asunis I, et al. Isolation of NF-E2-related factor 2 (Nrf2), a NF-E2-like basic leucine zipper transcriptional activator that binds to the tandem NF-E2/AP1 repeat of the beta-globin locus control region. *Proc Natl Acad Sci USA* 1994; 91: 9926–9930.
20. Gold R, Kappos L, Arnold DL, et al. Placebo-controlled phase 3 study of oral BG-12 for relapsing multiple sclerosis. *N Engl J Med* 2012; 367: 1098–1107.
21. Zu G, Zhou T, Che N, et al. Salvianolic acid A protects against oxidative stress and apoptosis induced by intestinal ischemia-reperfusion injury through activation of Nrf2/HO-1 pathways. *Cell Physiol Biochem* 2018; 49: 2320–2332.
22. Miao F, Wang R, Cui G, et al. Engagement of microRNA-155 in exaggerated oxidative stress signal and TRPA1 in the dorsal horn of the spinal cord and neuropathic pain during chemotherapeutic oxaliplatin. *Neurotox Res*. Epub ahead of print 23 April 2019.
23. Hall ED, Wang JA, Miller DM, et al. Newer pharmacological approaches for antioxidant neuroprotection in traumatic brain injury. *Neuropharmacology* 2019; 145: 247–258.
24. Nassenstein C, Kwong K, Taylor-Clark T, et al. Expression and function of the ion channel TRPA1 in vagal afferent nerves innervating mouse lungs. *J Physiol* 2008; 586: 1595–1604.
25. Caceres AI, Brackmann M, Elia MD, et al. A sensory neuronal ion channel essential for airway inflammation and hyperreactivity in asthma. *Proc Natl Acad Sci USA* 2009; 106: 9099–9104.
26. Bessac BF, Sivula M, von Hehn CA, et al. TRPA1 is a major oxidant sensor in murine airway sensory neurons. *J Clin Invest* 2008; 118: 1899–1910.
27. Trevisani M, Siemens J, Materazzi S, et al. 4-Hydroxynonenal, an endogenous aldehyde, causes pain and neurogenic inflammation through activation of the irritant receptor TRPA1. *Proc Natl Acad Sci USA* 2007; 104: 13519–13524.
28. Kim HJ, Wie J, So I, et al. Menthol modulates pacemaker potentials through TRPA1 channels in cultured interstitial cells of Cajal from murine small intestine. *Cell Physiol Biochem* 2016; 38: 1869–1882.
29. Griton M and Konsman JP. Neural pathways involved in infection-induced inflammation: recent insights and clinical implications. *Clinical autonomic research : official journal of the Clinical Autonomic Research Society* 2018; 28: 289–99.
30. Altenhofer S, Kleikers PW, Radermacher KA, et al. The NOX toolbox: validating the role of NADPH oxidases in physiology and disease. *Cell Mol Life Sci* 2012; 69: 2327–2343.
31. Salvemini D, Little JW, Doyle T, et al. Roles of reactive oxygen and nitrogen species in pain. *Free Radic Biol Med* 2011; 51: 951–966.
32. Lam GY, Huang J and Brumell JH. The many roles of NOX2 NADPH oxidase-derived ROS in immunity. *Semin Immunopathol* 2010; 32: 415–430.
33. Gavazzi G, Banfi B, Deffert C, et al. Decreased blood pressure in NOX1-deficient mice. *FEBS Lett* 2006; 580: 497–504.
34. Suzuki Y, Hattori K, Hamanaka J, et al. Pharmacological inhibition of TLR4-NOX4 signal protects against neuronal death in transient focal ischemia. *Sci Rep* 2012; 2: 896.
35. Kallenborn-Gerhardt W, Schroder K, Del Turco D, et al. NADPH oxidase-4 maintains neuropathic pain after peripheral nerve injury. *J Neurosci* 2012; 32: 10136–10145.